LINE BROADENINGS AND SHIFTS DURING THE IMPULSIVE PHASE OF FLARES

Ester Antonucci

Istituto di Fisica, University of Torino, Italy

INTRODUCTION

The thermal plasma formed during solar flares reaches temperatures between 1 -3 10^7K. In these conditions, the heavy elements of the solar atmosphere are highly ionized and emit soft X-ray (SXR) lines at short wavelengths down to 1 Å. Most of the space experiments devoted to solar studies flown in the past solar cycle, as for instance the Skylab spectrometers, obtained data for cool flare lines only; that is, for lines formed at temperatures below 10^7 K. An exception was represented by the Intercosmos-4 spectrometers which obtained the first high resolution SXR spectra in the region around 2 Å.

During the maximum of activity of the present cycle, three major experiments were devoted to the observation of this unexplored spectral region. High resolving power spectrometers were designed to detect mainly the highly ionized iron and calcium emission, in spectral regions with diagnostic properties, important to derive the physical conditions of flare plasmas. The most complex of these experiments, the Soft X-ray Polychromator, was flown on the Solar Maximum Mission (SMM) satellite. One of the two spectrometers which form the Soft X-ray Polychromator, the Bent Crystal Spectrometer, was especially designed to detect high temperature flare spectra with high time resolution. The spectrometer responds simultaneously in eight different SXR spectral regions. Spectrometers with comparable spectral resolution, but more limited spectral range and temporal resolution, were flown on the Airforce P78-1 and the Hinotori satellites.

Two important results on the dynamics of the thermal plasma during the explosive phase of flares have been obtained from the high resolution SXR spectra by studying line profiles. Large non-thermal broadenings and blue-shifted components are observed in flare lines. The first spectral property is related to the existence of significant turbulent, or random, mass motions, which originate at the time of the formation of the thermal plasma. Turbulence in flares in general precedes the major energy release and its possible relation to the acceleration mechanism itself is at the present investigated. Blue-shifted components in the

SXR spectra indicate that ascensional flows are present in the thermal plasma during the impulsive phase. These upflows indicate that high temperature plasma is transferred from the chromosphere into the active coronal loops. This process, known as chromospheric evaporation, occurs in response to localized heating of the chromosphere by electron beams or heat conduction during the impulsive energy release.

EXPERIMENTS FOR FLARE PLASMA OBSERVATIONS

The first high resolution solar spectra were detected in 1970 by Grineva et al. (1973). The iron lines between 1.85-1.87 Å were observed with two quartz spectrometers on board of the Intercosmos-4 satellite, launched on October 14, 1970. The spectra were obtained with a resolution of 4 10^{-4} Å, by scanning the solar disk with the satellite axis. The most important lines in the 1.85-1.87 Å were identified using these spectra (Grineva et al., 1973, Gabriel, 1972).

Systematic observations of spectral profiles of hot flare lines initiate, however, only during the last solar maximum with the Solflex (Solar Flares X-rays) experiment, consisting of 4 Bragg spectrometers operating in the interval 1.8-8.5 Å. The experiment was flown by NRL on an Air Force Spacecraft P78-1, launched on February 24, 1979 (Doschek et al., 1979). A wavelength scan is completed by this instrument in about 1 minute.

The Soft X-ray Polychromator, consisting of two instruments: the Bent Crystal Spectrometer (BCS) and the Flat Crystal Spectrometer (FCS), was flown on the SMM satellite on February 14, 1980. The experiment is described by Culhane et al., in the present issue. The BCS is formed by eight curved crystals and position sensitive detectors, to achieve an effective time resolution of 1 second, in the interval 1.7-3.2 Å. The Flat Crystal Spectrometer, with seven Bragg crystals which simultaneously diffract X-rays in seven different wavelength regions in the interval 1.4-22 Å, because of its imaging capabilities has obtained few spectroscopic data up to now.

Two rotating crystal spectrometers, SOX1 and SOX2, were flown on the Hinotori (Astro-A) satellite on February 21, 1981. The flat spectrometers scan simultaneously the two wavelength ranges 1.72-1.95 and 1.83-1.89 Å, by using the spin of the spacecraft itself (Tanaka et al., 1982). The time resolution is comparable to the effective time resolution of the BCS.

The spectrometers on the P78, SMM, and Hinotori satellites, have been operating continuously for many months, giving a large set of spectral observations of flare plasma at temperatures above 10^7 K.

HIGH TEMPERATURE SXR SPECTRA DURING THE IMPULSIVE PHASE OF FLARES

The spectral regions preferentially studied in the various experiments are the

wavelength bands near the resonance lines of helium-like iron (Fe XXV, 1.85 Å) and calcium (Ca XIX, 3.176 Å), where the satellite lines are formed. The intensity of such lines, which populate the longer wavelength side of the resonance line, are important in establishing the physical conditions of the flare plasma. The electron temperature can be determined by measuring the intensity of the dielectronic recombination satellites relative to the resonance line intensity and the plasma ionization conditions from the inner-shell transition satellite intensity (Gabriel, 1972). Figure 1 shows an example of flare spectrum in the region of the Ca XIX resonance line w, observed on May 9, 1980, with the BCS. Well-resolved satellite lines (indicated following the notation by Gabriel, 1972) are present at longer wavelengths, together with the intercombination and forbidden lines. Here, we

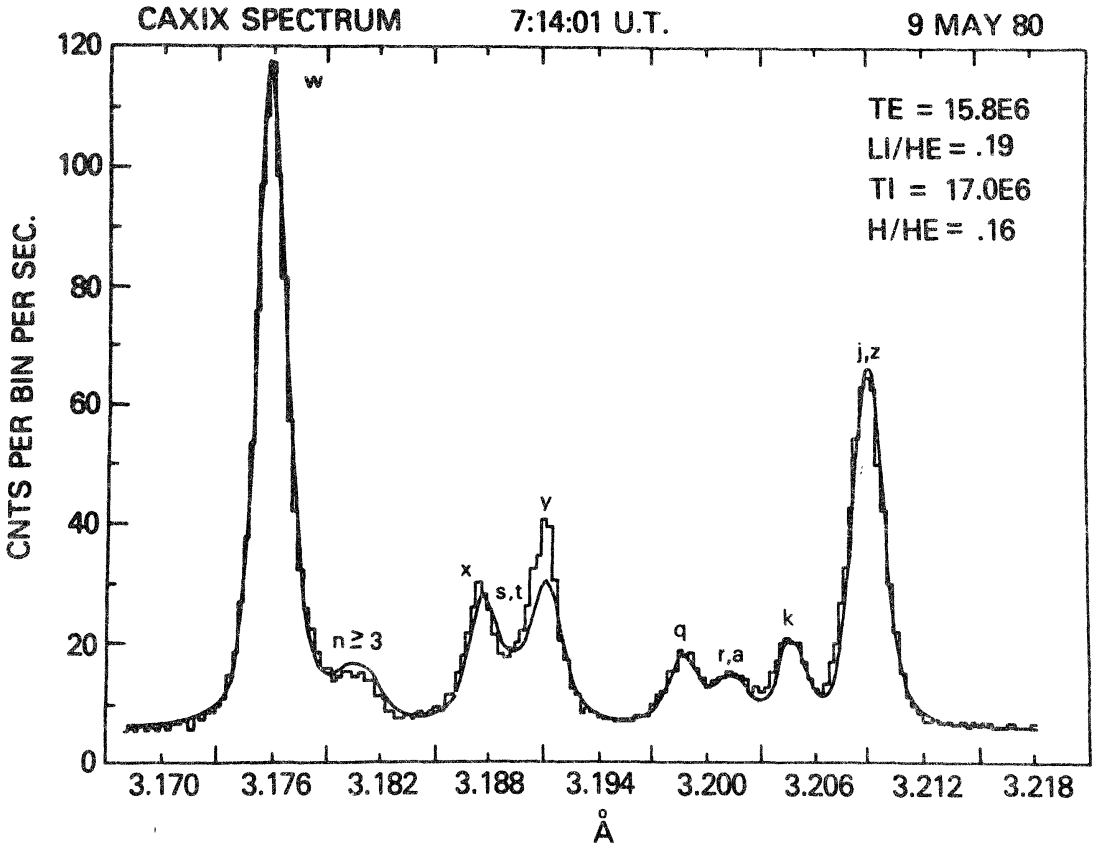

Figure 1. The Ca XIX spectrum observed at 07.14.01 UT, May 9, 1980, with the BCS is compared with a synthetic spectrum computed for an electron temperature of 1.58 10^7 K, a Doppler temperature of 1.7 10^7 K, a Li-He-like ion abundance ratio of 0.19 and H-He-like ion abundance ratio of 0.16. This spectrum is characteristic of the thermal phase of flares, since the lines are thermally broadened. The discrepancy between the theoretical and observed y line is of instrumental origin.

discuss primarily the information, derived from the analysis of SXR line profiles, on the dynamic conditions of the high temperature source and their temporal behavior.

The first observations of the Fe XXV resonance line, with the Intercosmos-4 satellite (Grineva et al., 1973), showed broad profiles, indicating turbulent motions of the order of 90 km s^{-1}. For the two spectra observed in the rise phase of a flare, the Fe XXV resonance line is shifted toward the blue; this implies a motion of the SXR source toward the observed with velocities of 160 km s^{-1}. Line shifts, observed during the peak or decay phase spectra, are toward the red and the down ward velocities deduced are of the order of 200 km s^{-1} (Korneev et al. 1980).

From the analysis of several flares of class M and X observed with the Solflex spectrometer, Doschek et al., 1980, and Feldman et al., 1980, conclude that line profiles are broader than the thermal width computed from the electron temperature determined with the dielectronic satellite method. Near the maximum X-ray flux the broadening decreases and in the decay phase lines are narrower. The line broadening at flare onset is characterized by a nonthermal velocity parameter of about 150 km s^{-1}. Two of the flares reported by Feldman et al., 1980, show in the rise phase a component of plasma moving outward from the sun at velocities of about 400 km s^{-1} and temperature near 1.5 10^7 K is observed. This result is based on the observation of a blue-shifted component in the calcium and iron SXR spectra. The blue-component is strongest in the earlier spectra and, after flare maximum, is either too weak to be measurable or absent. Wavelength shifts of the resonance line itself, as observed by Korneev et al., 1980, are not discussed by these authors. No obvious plasma flows such as just described are apparent in the spectra of class X flares, as discussed by Doschek et al., 1980.

The high time resolution observations of the flare SXR emission, obtained with the BCS on SMM, confirm that in the spectral range covering the emission of the Ca XIX and Fe XXV ions, the line profiles are broad and blue-shifted components are present. In addition, these two properties of the spectral lines have been systematically observed during the impulsive phase of the majority of class M and X flares (Antonucci et al., 1982). These line characteristics are more pronounced early in the flare when the rapidly changing line profiles can be better detected with a high time resolution spectrometer. The large set of impulsive phase spectra observed during SMM has enabled to derive a rather extensive description of random and bulk motions in the flare plasma. The relative timing of plasma flows and energy deposition, the physical properties of plasma flows, and their location at least at flare onset have been determined, enabling a comparison with the models proposed to explain the SXR flare plasma (Antonucci, 1982; Antonucci and Dennis, 1983; Antonucci et al., 1984 a and b).

The results obtained from the Hinotori observations are in general confirming the existence of non-thermal profiles and blue wings of spectral lines. Non-thermal velocities of about 200 km s^{-1} and upward velocities of about 400 km s^{-1} are derived at flare onset (Tanaka et al., 1982).

The sequence of calcium spectra detected during the May 21, 1980 flare, in Figure 2, illustrates the changes in spectral line profiles observed during the impulsive phase. The first significant SXR emission detected in the spectral band from 3.165 to 3.231 Å, where the Ca XIX resonance line and its satellites are observed, in Figure 2 a, is an average over 120 seconds. The emission is integrated over the entire flare region, since the BCS field of view is 6' x 6'. The resonance line is significantly broadened with a Doppler temperature of about 1.3 10^8 K. This broadening must be non-thermal in origin since it would imply an ion temperature of an order of magnitude larger than the electron temperature of about 9 10^6 K. Hence, turbulent motions with a mean velocity of 220 km s^{-1} are expected in the flaring region.

The subsequent spectrum, in Figure 2 b, shows the appearance of a blue-shifted component, the most relevant feature being at the blue side of the resonance line of the main spectrum. The two lines have comparable intensities and the relative blue-shift of the new feature is 3.8 mÅ, value which implies high speed plasma flows with line-of-sight velocity of about 370 km s^{-1} relatively to the principal source. The line-of-sight is approximately radially outward since the flare occurred near disk center at S14 W15. In the spectrum of Figure 2 c, the blue-shifted emission decreased in intensity relative to the unshifted component with unchanged line-of-sight velocity. The line spectrum continues to consist of two components until the SXR emission reached its peak intensity at 21.07 UT. After this time, blue-shifts are absent as well as the non-thermal excess in line profiles. Figure 2 d shows an example of one-component spectrum with thermal line profiles, characteristic of the flare peak and decay phases.

The principal resonance line, during the early stages of the flare, is itself blue-shifted with respect to the rest wavelength during the late impulsive and cooling phases, indicated with a vertical dashed line, in Figure 2. The shift of the order of 0.8 mÅ, corresponds to a flow velocity of about 80 km s^{-1}.

Synthetic spectra which best fit the data, are shown as continuous lines superposed to the observed counting rates, in Figure 1 and 2. These theoretical spectra are obtained from a synthesis of lines computed for a given set of physical parameters of the source, such as electron temperature and ionization conditions. Lines are then convolved with a gaussian profile to allow for both thermal and random motions and a lorentzian profile to account for the crystal response. This methods, has been developed to analyse high temperature SXR spectra by Antonucci et al. (1982). The atomic parameters used for deriving synthetic spectra and the diagnostic properties of satellite lines are described in this issue by Bely-Dubau and Gabriel. The two component spectra, observed when blue-shifted lines are emitted by the high velocity plasma, are fitted by the sum of two spectra, synthesised for the same source parameters.

GENERAL PROPERTIES OF THE PLASMA MOTIONS

The analysis of a large set of flare spectra observed with the BCS during 1980 enables to describe the behaviour of the stationary and dynamic components of the SXR flare plasma during the impulsive phase (Antonucci et al., 1984a). Blue-

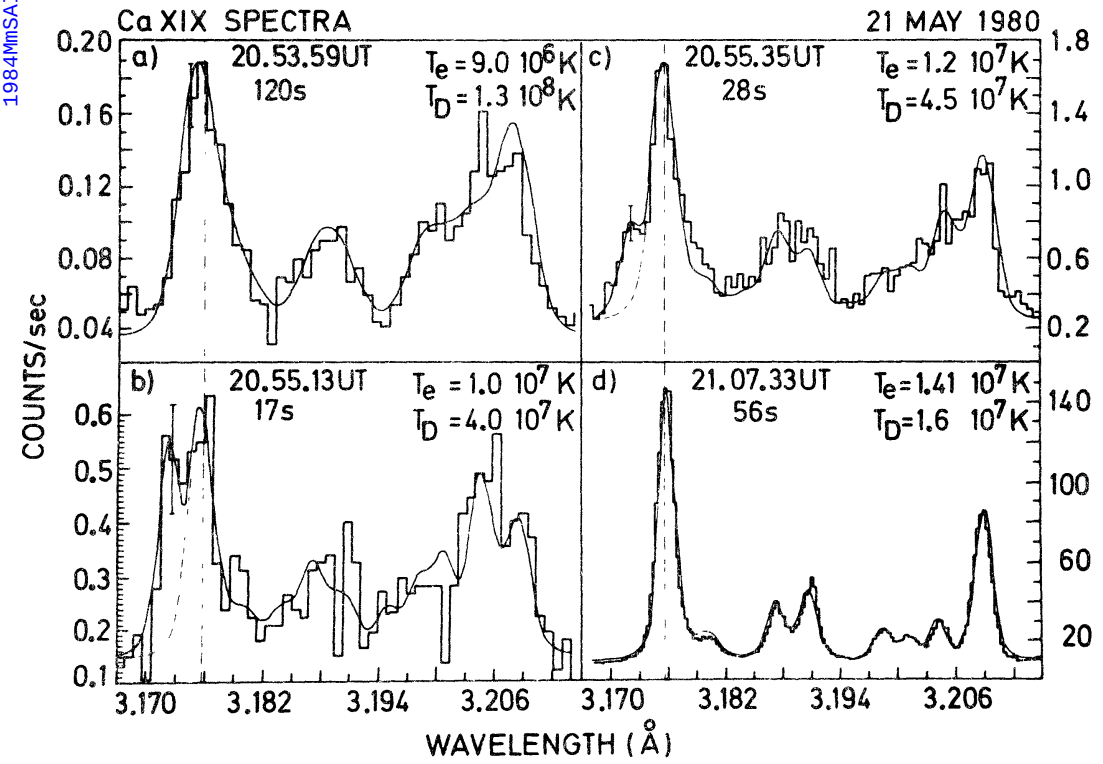

Figure 2. Sequence of soft X-ray spectra obtained at four different times during the impulsive phase of the May 21, 1980 solar flare with the BCS in the Ca XIX spectral region. The smooth curve in each figure represents the synthesized spectrum computed for given values of the electron temperature T_e and the Doppler temperature T_D. The spectra shown in b and c are the sum of two synthetic spectra, one blue-shifted by 3.8 mÅ. The dashed lines represents the profile of the principal component expected for the given Doppler temperature. The time of the spectra are the mean times of the observation intervals.

shifted components are observed throughout the impulsive phase in the majority of disk flares. The absence of blue shifted components in flares located beyond 60 degrees in longitude, indicates that flows in the SXR plasma are mainly outward. Upward velocities are of 300-400 km s^{-1} at flare onset. In the decay phase, the dynamic component in the SXR source is no longer observed (shifts between spectral components corresponding to velocities below 120 km s^{-1} cannot be measured reliably). In both disk and limb flares, large non-thermal line broadenings are observed, and the non-thermal line broadening is not strongly dependent on the position of the flare on the solar disk. Lines are in general thermal in the decay phase.

Upflows are observed simultaneously to the most intense hard X-ray (HXR) emission and to the rise of the SXR emission. This indicates a causal relation of these three phenomena. SXR and HXR emission from the region of the April 8 1980 flare are shown in Figure 3 as an example. The HXR emission is measured with the Hard X-ray Burst Spectrometer (HXRBS) on SMM (Orwig et al., 1980). Defining the parameter ΔT, difference between the Doppler and electron temperatures, as an indicator of the non-thermal broadenings, and defining v' as the velocity of the dynamic component of the SXR source, it can be seen that these quantities deviate considerably from zero during the impulsive HXR emission and the rise of the SXR flare, as shown in Figure 3. Both quantities moreover are large at flare onset and decrease during the impulsive phase. If non-thermal broadenings are interpreted as due to the turbulent conditions of the flaring plasma, it is concluded that both velocities of the bulk and turbulent motions decrease with time from flare onset to negligible values at flare maximum. In some flares, the main component is broadened one or two minutes before the blue-component is observed.

While the upflow velocity is decreasing, the density in the coronal region of the flare is increasing, as can be deduced from the evolution of the emission measure EM of the stationary SXR source. For the April 8 event, the quantity log (EM) is shown in Figure 3. Since the area of flares as observed in soft X-rays with the Hard X-ray Imaging Spectrometer (HXIS) on SMM (the instrument is described by Van Beek et al., 1980) does not change significantly during most of the impulsive phase, the increase in EM indicates a simultaneous increase in electron density in the flare plasma.

The emission of high speed upflows is in general weaker than that of the main SXR source, except for a short period, of the order of 20 seconds, at flare onset, when the intensity of the blue- shifted emission is observed to be equal to that of the primary emission, as for example in Figure 2. This is however observed in a few cases.

The blue shift of the principal resonance line at flare onset observed in a number of events, as reported by Korneev et al., 1980, and in the discussion of Figure 2 for the May 21 event, is interpreted as an initial upward motion of the entire SXR source. The upward velocity is of about 100 km s^{-1} or less. This motion precedes the appearance of high speed upflows, evidenced by the blue-shifted component. In the slowly moving SXR plasma turbulent mass motions show the highest velocities during the flare. Blue-shifts are observed later in coincidence with a significant increase in the rise of the HXR emission. The threshold value for the energy input flux into the chromosphere to initiate high speed upflows is estimated to be 10^{10} erg s^{-1} cm^{-2} (Antonucci et al., 1984a).

LOCATION OF MASS MOTIONS AT FLARE ONSET

The SXR and HXR images, detected respectively in the 3.5-8 keV and 16-30 keV energy bands of the HXIS, enable to locate the sites where upflows originate. The HXIS, with a spatial resolution of 8", in a few cases has resolved separate HXR sources at flare onset. These sources have been identified with the foot-

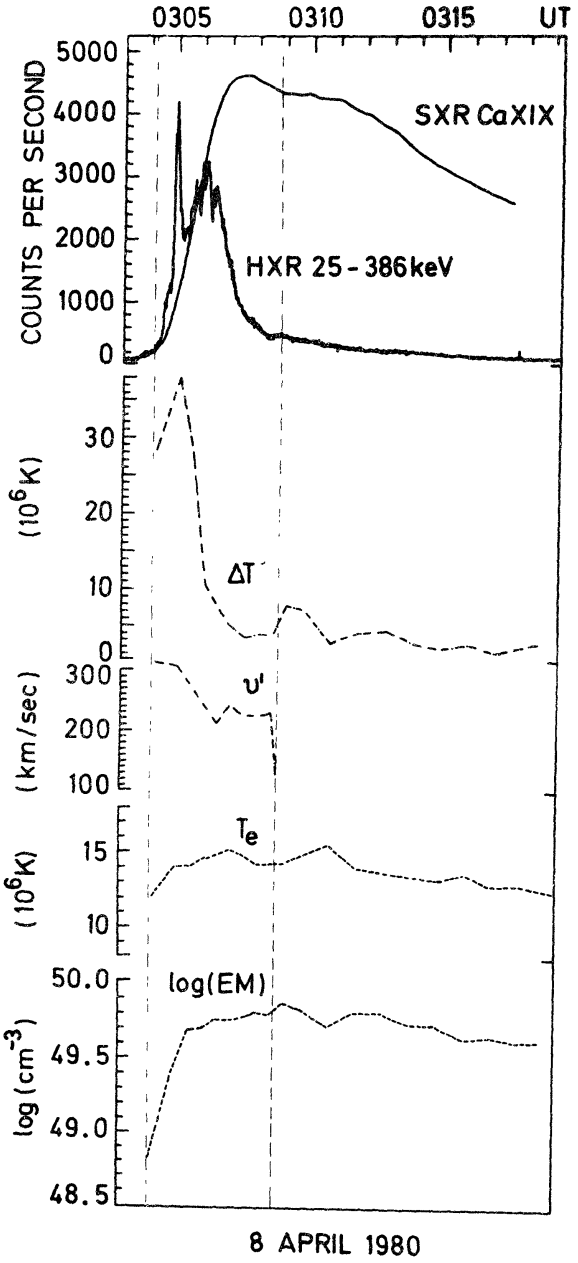

Figure 3. Temporal evolution of the following quantities for the flare on April 8, 1980: the soft X-ray emission SXR integrated over the spectral range 3.165 to 3.231 Å, the hard X-ray emission HXR detected with the HXRBS in the energy range from 25 to 386 keV, the difference in Doppler and electron temperatures ΔT, the velocity v' of the high speed upflows, the electron temperature Te, and the logarithm of the emission measure log (EM) of the principal soft X-ray source. The last four physical parameters were derived from the analysis of BCS Ca XIX spectra similar to those shown in Figure 1 and 2. High speed upflows are observed during the time interval delimited by the dashed vertical lines.

points of the flaring loops (Hoyng et al., 1981, Duijveman et al. 1982). In fact, the HXR bright points are known to be associated with regions of opposite magnetic polarities and have been interpreted as caused by the incidence in the chromosphere of beams of particles accelerated during the primary energy release. The images observed during the May 21 event, shown in Figure 4, indicate that at the time of the appearance of the high speed mass flows (Figure 2b) the SXR emission is concentrated mainly at the sites A and B, which correspond to the HXR sources at the footpoints of coronal loops. Hence, since SXRs are mainly from A and B, it is possible to infer that high speed plasma upflows originate at the sites of local chromospheric heating. Another consequence is that the high velocity random mass motions develop also in the sites of energy deposition (Antonucci et al, 1984b).

ENERGETICS OF THE IMPULSIVE PHASE UPFLOWS

The general properties derived from the observations of systematic upflows during the rise phase of SXR flares, are qualitatively consistent with the hypo-

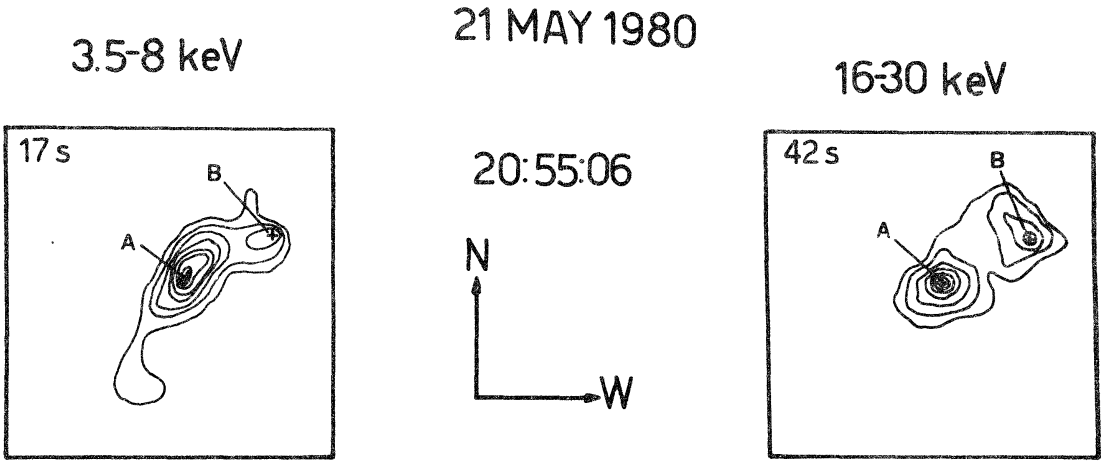

Figure 4. X-ray images of the flaring region, during the May 21, 1980 event, in the softer (3.5-8 keV) and harder (16-30 keV) energy bands of the HXIS. The initial time of the images correspond to the start of the high speed upflows; the soft X-ray image is accumulated over 17 seconds and the hard X-ray image over 42 seconds. The crosses represent the peak of the hard X-ray emission at the two footpoints A and B.

thesis of chromospheric evaporation. Under this hypothesis, plasma upflows are the manifestation of chromospheric material impulsively heated and driven up along the magnetic field lines to fill the flaring coronal loops, where the stationary SXR source then forms. Upflows are expected to originate at the sites of energy deposition, that is at the footpoints of coronal loops. If the HXR impulsive emission is a temporal indicator of energy deposition in the chromosphere, upflows are expected until the impulsive HXR emission is observed. Local chromospheric heating and impulsive HXR emission are both a direct consequence of the primary energy release and both can be produced either by electron beam heating or conduction heating of the chromosphere. While evaporation takes place, the plasma accumulating in a magnetically confined coronal region, the stationary SXR source, is expected to increase. The velocity of the evaporating plasma has to decrease with the increase in density of the plasma accumulating in the coronal region, because of the decrease in pressure difference between the chromosphere and the overlying coronal flare loop. All these characteristics are indeed consistent with the results presented in the two previous sections.

For a definitive identification of upflows with chromospheric evaporating material, it should be proved that upflows can quantitatively account for the formation of the SXR source in the coronal region. However, the amount of thermal plasma supplied to the corona by the upflows cannot be directly established, since the amount of mass, enthalpy and kinetic energy flowing into the coronal region, cannot be precisely determined from the observations. Nevertheless, it is possible to determine under which conditions the observed plasma upflows are consistent with the increase in coronal plasma, in the assumption that they are continuous and magnetically confined. This is done by determining the average density and temperature of the evaporating material, required to supply sufficient mass and energy to the coronal SXR source during the evaporation process. The total energy input to the SXR source corresponds to the sum of the thermal and turbulent energy increases and of the integral losses for conduction and radiation from the coronal region since flare onset.

The electron temperature and density derived for the upflows, for a set of well-observed flares, are of the order of those observed in the coronal SXR source at the end of evaporation. Since for the upflows these quantities represent lower limits, they are consistent with the requirement that the pressure in the evaporating plasma must exceed the pressure at the top of the loop, to fill the magnetic loops. Therefore, under the conditions that their density is equal or greater than $1\ 10^{11}$ cm^{-3} and their temperature is of the order of $1\text{-}2\ 10^{7}$ K, the plasma upflows observed during the rise of the SXR coronal emission, can indeed supply the coronal plasma observed during the peak phase of the SXR flare (Antonucci, et al., 1984a).

NUMERICAL SIMULATIONS OF THE HYDRODYNAMIC RESPONSE OF A CORONAL LOOP TO IMPULSIVE HEATING

Numerical simulations have been developed by several authors to model the hydrodynamic response of a coronal loop, given an initial impulsive heating. All of them predict chromoshperic evaporation although with different characteristics. In a

number of calculations, chromospheric heating is assumed to be due to collisions by non-thermal electrons of a given flux (e.g. Somov et al., 1981; Mac Neice et al., 1983; Fisher et al., 1984). In other models, the flux tube is heated in a localized region, according to a given heating function and chromospheric evaporation is driven by conduction (e.g. Somov et al., 1982; Cheng et al., 1983; Pallavicini et al., 1983). For beam heating, the hydrodynamic response of the chromosphere is different depending on the energy input flux (Fisher et al., 1984). For an energy input flux below a threshold of about 10^{10} erg cm^{-2} s^{-1}, a "gentle" evaporation is induced at moderately low speed. Above this threshold, the chromospheric material rapidly heats up to coronal temperatures with a consequent explosive expansion into the corona. The overpressure created in the chromosphere by the impulsive heating has not only the effect of driving heated material upwards, but also mass downwards into the chromosphere. In the case of evaporation driven by conduction, the flow velocities are lower than those predicted for explosive evaporation, which are typically twice the sound speed in the evaporating material.

While the observed upflow velocities, for class M and X flares, are in general consistent with the values predicted for evaporation driven by conduction, the sudden transition from slow to high speed flow velocities, observed in coincidence with the impulsive increase in energy input rate, is in better agreement with the two-regime evaporation predicted in the case of beam heating. The observed value of the energy input rate threshold, corresponding to a change in the evaporation regime, is also in agreement with the value predicted by Fisher et al., 1984. Hence, although in principle the observational properties of chromospheric evaporation should enable to distinguish between the two main mechanisms suggested for chromospheric heating during the energy release, at the present this is not yet feasible.

One of the models of chromospheric evaporation (Doschek et al., 1983; Cheng et al., 1983) not only predicts the density, temperature and velocity along the flaring flux tube, but also the line intensities and profiles that would be observed by an instrument with a field of view including the entire loop. This enables to compare directly the predicted line profile and intensity with the observations. In this model the conservation equations of mass, momentum and energy are solved numerically for a two fluid plasma, consisting of electrons and protons. Heating is localized at the top of the loop; therefore evaporation is driven by conduction. The effect of evaporation on the spectral lines is the following.

Chromospheric and transition region lines, below 10^6 K, are red-shifted by a small amount, corresponding to downward velocities of 20 km s^{-1}. Coronal lines with temperatures within 1-3 10^6 K remain unshifted. Flare lines are blue-shifted with upward velocity around 200-400 km s^{-1}. The results of this simulation show that at flare onset, the blue-shifted component should be dominant in the spectrum. As evaporation proceeds, the ratio of the blue-shifted to the stationary component decreases until the stationary component dominates. This picture is however significantly modified for asymmetric heating of the coronal loop (Cheng et al., 1984). The predicted line profiles, in this case, are more complex. Both blue and red-shifts are expected and their relative importance depends also on the loop orientation with respect to the observer.

Although the general predictions for high-temperature flare lines are consistent with the observations, a detailed comparison between numerical results and observations does not yet give significant indications, since the initial conditions of the loop, or loops, the form of the heating function, the geometry of the magnetic region are poorly known. A number of groups are at the present involved in the effort of improving the hydrodynamic simulation of flaring loops with complex configurations, and considerable progress is expected in this field. A complete review of the state of flare loop modelling will be published on the SMM Workshop proceedings by Kopp et al., 1984. (see also Kopp in this issue).

ORIGIN OF NON-THERMAL LINE PROFILES

The non-thermal broadening of X-ray lines is commonly attributed to mass motions, since the observed profiles would imply a difference in ion and electron temperatures sometimes exceeding one order of magnitude. At the density inferred for the thermal plasma of flares, however, it would be difficult to explain the persistence of large differences in electron and ion temperatures over the observed flare rise times.

If the non-thermal line profiles are indeed caused by mass motions, then the question is whether these are random, or magnetically driven, or convective motions with a complex velocity distribution, associated with the evaporation process. Both the correlation existing between the maximum upflow velocity during evaporation and the maximum turbulent velocity, indicating the non-thermal excess in line profiles, and the temporal correlation of upflows and line-broadenings are in favour of interpreting broad profiles as a consequence of the presence of convective velocities in flaring loops. If the flare heating and the loop geometry are asymmetric, then downflows are predicted as well as upflows. The result on line profiles is the following upflows and downflows should be observed simultaneously with a stronger upward component for disk flares, giving origin to broad lines with blue wings. At the limb, the upflow excess should disappear and spectral lines should appear somewhat broader. A number of simulations have also shown the importance of considering complex configurations of magnetic loops, with different projection angles; in each case broadenings produced by evaporation are predicted. A detailed description of these studies is given by Doschek et al.(1984), as a result of the SMM Workshop.

The main spectral component is, however, broadened before the high speed upflows are measurable in the flaring loops. At this time the SXR emission is close to the loop footpoints. In addition, the degree of broadening is not strongly dependent on the position of the flare on the disk. Both facts suggest that, although the broadening may be in part due to the convective velocity distribution, there has to be a contribution to the effect which is independent of evaporation and this contribution is predominant at flare onset. In the example of the May 21 event, discussed before, it is possible to distinguish clearly a flare phase, with moderate chromospheric heating preceding the impulsive rise in energy release, during which random motions are dominant. This is not an unique case and suggests that turbulent motions may be associated with the mechanism responsible for the particle acceleration in flares.

SOMMARIO

Gli spettrometri ad alta risoluzione operanti durante il recente massimo di attività solare hanno permesso di ottenere per la prima volte accurate osservazioni di righe di emissione del plasma che si forma durante i brillamenti solari. Durante tali fenomeni, il plasma coronale raggiunge temperature superiori ai 10^7 K. Gli spettri emessi nella fase esplosiva del brillamento sono caratterizzati da righe dal profilo considerevolmente allargato e da componenti spostate verso il blu. Se ne deduce l'esistenza di moti sia turbolenti, sia ascensionali, nel plasma che emette raggi X. I moti turbolenti sono probabilmente legati al processo stesso di accelerazione. I moti ascensionali indicano che il plasma ad alta temperatura si forma per accumulazione nella corona di materiale cromosferico, che, riscaldato localmente all'inizio del brillamento, evapora lungo le linee di campo magnetico dei loop coronali.

REFERENCES

Antonucci, E., et al., 1982, Solar Phys., 78, 107.

Antonucci, E., 1982, Mem. S.A.It., 53, 495.

Antonucci, E., Dennis, B.R., 1983, Solar Phys., 86, 67.

Antonucci, E., Gabriel, A.H., Dennis, B.R., 1984a, Ap.J., in press.

Antonucci, E., Gabriel, A.H., Dennis, B.R., 1984b, Solar Phys., submitted.

Cheng, C.-C., Oran, E.S., Doschek, G.A., Boris, J.P., Mariska, J.T., 1983, Ap.J., 265, 1090.

Cheng, C.-C., Karpen, J.T., Doschek, G.A., 1984, Ap.J., submitted.

Doschek, G.A., Kreplin, R.W., Feldman, U., 1979, Ap.J. 233, L157.

Doschek, G.A., Feldman, U., Kreplin, R.W., Cohen, L., 1980, Ap.J. 239, 725.

Doschek, G.A., Cheng, C.-C., Oran, E.S., Boris, J.P., Mariska, J.T., 1983, Ap.J., 265, 1103.

Doschek, G.A., et al., 1984, Proceedings of the SMM Workshop, in preparation.

Duijveman, A., Hoyng, P., Machado, M.E., 1982 Solar Phys., 81, 137

Feldman, U., Doschek, G.A., Kreplin, R.W., Mariska, J.T., 1980, Ap.J. 241, 1175.

Fisher, G.A., Canfield, R.C., McClymont, A.N., 1984, Ap.J., in press.

Gabriel, A.H., 1972, Mon. N. R. astr. Soc., 160, 99.

Grineva, U.I., et al., 1973, Solar Phys., 29, 441.

Hoyng, P., et al., 1981, Ap.J., 246, L155.

Kopp, R., et al., 1984, Proceeding of the SMM Workshop, in preparation.

Korneev, V.V., Zhitnik, I.A., Mandelstam, S.L., Urnov, A.M., 1980, Solar Phys. 68, 391.

MacNeice, P., McWhirter, R.W.P., Spicer, D.S., Burgess, A., 1984, Solar Phys., 90, 357.

Orwig, L.E., Frost, K.J., Dennis, B.R., 1980, Solar Phys., 65, 25.

Pallavicini, R., Peres, G., Serio, S., Vaiana, G., Acton, L.W., Leibacher, J.W., Rosner, R., 1983, Ap.J. 270, 270.

Somov, B.V., Syrovatskii, S.I., Spector, A.R., 1981, Solar Phys. 73, 145.

Somov, B.V., Sermulina, B.J., Spektor, A.R., 1982, Solar Phys., 81, 281.

Tanaka, K., Watanabe, T., Nishi, K., Akita, K., 1982, Ap.J., 254, L59.

Van Beek, H.F., Hoyng, P., Lafleur, B., Simnett, G.M., 1980, Solar Phys., 65, 39.